Parametric Point Spread Function Estimation for Thermal Imaging Systems using Easy-to-Manufacture Random Pattern Targets

Florian Piras[a], Edouard De Moura Presa[b], Peter Wellig[b], and Michael Liebling[a,c]

[a]Idiap Research Institute, Martigny, Switzerland
[b]armasuisse Science and Technology, Thun, Switzerland
[c]University of California, Santa Barbara, CA, USA

ABSTRACT

Thermal and visible cameras can be characterized by their point spread function (PSF), which captures the aberrations induced by the image formation process, which includes effects due to diffraction or motion. Various techniques for estimating the PSF based on a simple image of a target object that consists of a random pattern were shown to be effective. Here, we describe a computational pipeline for estimating parametric Gaussian PSFs characterized by their width, height, and orientation, based on binary random pattern targets that are suitable for thermal imaging and easy to manufacture. Specifically, we consider the influence of deviating from a strict random pattern so the targets can be manufactured with common cutting or 3D printing devices. We evaluate the estimation accuracy based on simulated patterns with varying dot, pitch, and target sizes for different values of the point spread function parameters. Finally, we show experimental examples of acquired on manufactured devices. Our results indicate that the proposed random pattern targets offer a simple and affordable approach to estimating local PSFs.

Keywords: deconvolution, thermal imaging, artifact removal

1. INTRODUCTION

The point spread function (PSF) of an imaging system conveys key information both about the instrument and the imaging conditions. It models the response of an imaging system to an ideal point source of light. In perfect imaging conditions, the PSF can help characterize a camera's performance based on features like its focal length and aperture. In more complex imaging situations, like when athmospheric conditions are variable or when objects are moving in the scene or are located at different distances, the PSF will change, possibly raising the need for having different PSF's in different regions of the image to accurately model the image formation process. Knowledge of the PSF in various regions of an image may also convey information about focus, which in turn could be used to infer depth.[1] The optical image formation model, a convolution of an ideal image with the PSF,[2] is largely similar across imaging fields, from microscopy to astronomy, and can be adapted to take into account magnification or various wavelength ranges. Parametric models of the PSF based a decomposition of the optical pupil function in Zernicke polynomials[2] have been proposed, but also simpler models, like approximations by a 2D Gaussian function, were shown to be of practical use in some domains.[3]

There are multiple methods for determining an imaging system's PSF. The ill-posedness of the estimation problem has been studied by Ehret *et al.*[4]

The idea of using a random chart and of modeling the point spread function with simple Gaussians was proposed by Kubota and Ohzu.[5] Brauers *et al.* have proposed a direct PSF estimation method that uses a random noise target and to estimate a non-parametric PSF in local areas.[6] Levy *et al.* a proposed a modulation transfer function estimation method for lenses that use random targets.[7]

There are multiple methods available to directly estimate the PSF in naturally-occurring images based on a regression algorithm trained on a large set of natural images. Proposed methods use convolutional neural

Further author information: florian.piras@idiap.ch

To cite this paper:
Florian Piras, Edouard De Moura Presa, Peter Wellig, Michael Liebling, "Parametric point spread function estimation for thermal imaging systems using easy-to-manufacture random pattern targets," Proc. SPIE 13199, Target and Background Signatures X: Traditional Methods and Artificial Intelligence, 1319905 (1 November 2024); https://doi.org/10.1117/12.3031519

network (CNN)'s and model the PSF as either a decomposition of the optical transfer function in terms of Zernicke polynomials or Gaussians.[8] The latter approach has also been applied to thermal imaging,[9] where the method's performance was found to be better if the images contained a wide variety of frequencies (textures).

In this paper we focus a method for determining the PSF of an imaging system in a local area, based on the acquisition of an image of a target that exhibits a pattern generated by a random process such as a normal or binomial distribution. The Fourier transform images of such patterns retains a random nature, for example, a pattern generated by a normal process transforms to a pattern that also follows a normal distribution in the frequency domain. Furthermore, since the imaging process is modeled by the convolution of the pattern with the PSF, in the frequency domain, the operation corresponds to a multiplication of the pattern and the PSF's Fourier transforms. Detecting the envelope, in frequency space, of the resulting pattern gives direct access to the PSF characteristics. Despite the simplicity of the theory, in practice, several difficulties arise in practice, including the periodic nature of the discrete version of the Fourier transform, the fast Fourier transforme (FFT), and the problem of estimating the PSF's parameters lends itself to many variations. Here, we report on an implementation that pipeline that takes into account these practical considerations, and the practical constraints of generating pattern that only follow the idealized patterns approximately. We further describe a physical implementation, consisting of a laser-cut test target, to make the method suitable for thermal imaging.

This paper is organized as follows. In Section 2, we recall the theory for the determination of the PSF and the pipeline we implemented. In Section 3, we present experiments that characterize the method based on simulated patterns, to evaluate the impact of approximate implementation of the idealized method or the robustness to additive noise. We further illustrate the method with a practical example. Finally, we discuss the results in Section 4 and conclude in Section 5.

2. METHODS

2.1 Theory

We briefly recall the key mathematical derivations that lead to our method. A convolution operation between two functions $f(x, y)$ and a convolution kernel $h(x, y)$ in space corresponds to a multiplication in the frequency domain:

$$f * h(x, y) \overset{\mathcal{F}}{\longleftrightarrow} \hat{f}(\omega_x, \omega_y) \cdot \hat{h}(\omega_x, \omega_y). \tag{1}$$

Furthermore, the Fourier transform of a two-dimensional (2D) *white noise* signal $w(x, y)$, whose samples follow a normal distribution with standard deviation σ is, again white noise:

$$w(x, y) \sim \mathcal{N}(0, \sigma) \overset{\mathcal{F}}{\longleftrightarrow} \hat{w}(\omega_x, \omega_y) \sim \mathcal{N}(0, \sigma), \tag{2}$$

that is, the power distribution over the entire spectrum is *flat*.

Combining Equations (1) and (2), the Fourier transform of white noise convolved with a PSF $h(x, y)$ is:

$$w * h(x, y) \sim \mathcal{N}(0, \sigma) \overset{\mathcal{F}}{\longleftrightarrow} \hat{w}(\omega_x, \omega_y) \cdot \hat{h}(\omega_x, \omega_y), \tag{3}$$

where we notice that, because the power distribution of $\hat{w}(\omega_x, \omega_y)$ is flat, the envelope of the product corresponds to $\hat{h}$.

Before reaching our final result, we recall that the Fourier transform of a Gaussian function is, again, a Gaussian function:

$$g(t) = \gamma \mathrm{e}^{-\alpha t^2} \overset{\mathcal{F}}{\longleftrightarrow} \hat{g}(\omega) = \gamma \sqrt{\frac{\pi}{\alpha}} \mathrm{e}^{-\omega^2/(4\alpha)} \tag{4}$$

and that the Fourier transform of a 2D function, after it has undergone an affine transformation, defined by $\mathbf{x}' = A\mathbf{x}$ is:

$$f(\mathbf{A}\mathbf{x}) \overset{\mathcal{F}}{\longleftrightarrow} \frac{1}{\det(\mathbf{A})} \hat{f}\left((\mathbf{A}^{-1})^{\top} \boldsymbol{\omega}\right). \tag{5}$$

We model the PSF as rotated 2D Gaussian with 3 parameters

$$h(x, y) \approx g(x, y) \quad \text{with parameters:} \sigma_x, \sigma_y, \theta, \tag{6}$$

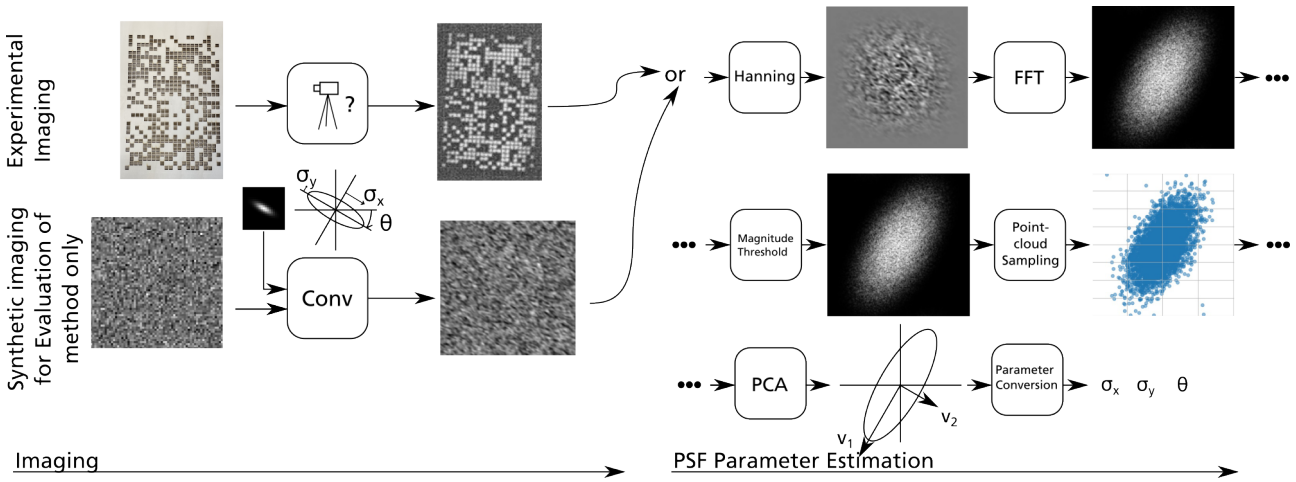

Figure 1: Flowchart of the PSF parameter estimation method.

where the parameters σ_x, σ_y define the variances in x and y and θ a rotation angle. Our goal is to estimate these parameters, based on a measurement of $w * h(x, y)$ in Equation (3). Our approach consists in generating a set of points in the frequency domain with a spatial distribution that corresponds to the shape of the above envelope. Since the shape of this distribution is that of a centered 2D Gaussian whose parameters are inversely proportional to those of the PSF, we can estimate these parameters via a principal component analysis (PCA).

2.2 Algorithm

The above theoretical derivation leads to the following algorithm summarized in Fig. 1.

1. Capture image of a pattern whose grayscale values are distributed according to a normal distribution.
2. Apply a Hanning window weighting, which allows mitigating the contribution from the periodic boundary conditions that are implicitly assumed in the FFT step.
3. Compute the two-dimensional FFT.
4. Perform a soft-threshold of the FFT coefficients to attenuate the effect of noise.
5. Generate N vectors $\vec{\omega}^n = (\omega_x^n, \omega_y^n)^\top$ with a random generator such that that their frequency distribution matches that of the discrete FFT in the previous step. The vectors define the position of points in the frequency space, and are gathered in an $N \times 2$ matrix X whose N rows contain the N vectors $X_n = (\vec{\omega}^n)^\top$.
6. Compute the PCA on this matrix. The calculated PCA components correspond to the best match of an idealized 2D Gaussian window to the PSF's Fourier transform. The PCA results in two perpendicular vectors $\vec{v}_1$ and $\vec{v}_2$, with $\vec{v}_1$ oriented along the direction of the greatest variance of the point distribution, and with vector lengths corresponding to the distribution's variances σ_{ω_x} and σ_{ω_y} and with the vector direction indicating the inclination θ.
7. Transform the parameters of the estimated distribution in the spectral domain to parameters in the spatial domain according to: $\sigma_x = \dfrac{M}{2\pi\sigma_{\omega_x}}$ and $\sigma_y = \dfrac{M}{2\pi\sigma_{\omega_y}}$, where M is the size of the $M \times M$ image, in pixels.

3. RESULTS

3.1 Evaluation of the PSF estimation method

We evaluated the PSF estimation algorithm on patterned target images obtained by either generating a *Gaussian process pattern target* by generating grayscale values according to a normal distribution and a *binomial pattern target* by generated binary values based on a binomial distribution. The two patterns are shown in Figure 2.

We then convolved these target with synthetic PSF's of various parameters σ_x, σ_y and inclinations θ to obtain blurred targets to which we applied the PSF estimation method. Specifically, we set $\sigma_y = 1$, and varied the ratio $r = \sigma_x/\sigma_y$ in the range $[1, 8]$ yielding values of σ_x in the same range. We varied θ in the range $-89°$ and $90°$.

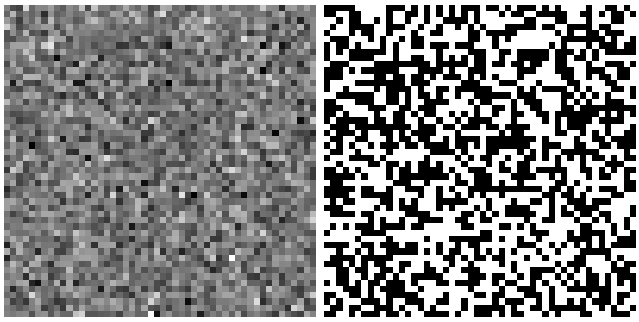

(a) Gaussian process pattern (b) Binomial pattern

Figure 2: Generated pattern used for simulation.

3.1.1 Gaussian process patterns

We set the size of Gaussian process pattern target to 201×201 pixels. In Figure 3, top, we investigated the errors between ground truth and estimated parameters σ_x, σ_y and θ. An example of the synthetically blurred target for a given PSF parameter combination is shown, along with the PSF and its estimate. In Figure 3, bottom, we repeated the estimation method's robustness to additive noise. To this end, we added 1% of Gaussian noise to the synthetic image.

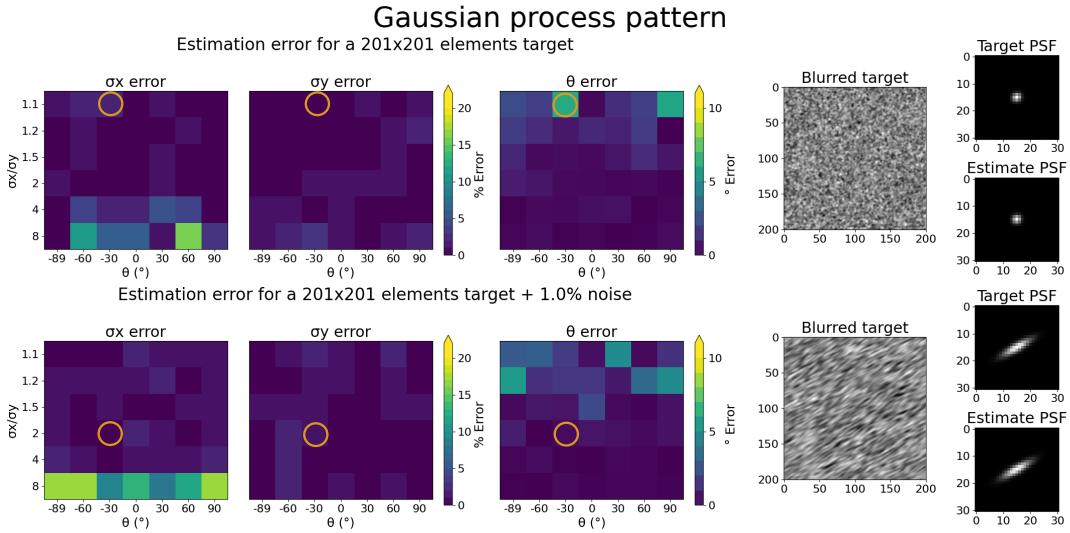

Figure 3: Evaluation of the method for Gaussian process pattern of size 201×201 pixels, blurred with $\sigma_y = 1$, $\sigma_x = \sigma_y \times r$, with ratio $r = \sigma_x/\sigma_y$, and θ in the range of $-89°$ to $90°$. The errors in the estimation of the parameters σ_x, σ_y are given in percent, and the error in estimating θ in degrees. An example of synthetically-generated blurred image, PSF and corresponding estimate are shown on the right for parameters in the orange circles. Top and bottom rows are without and with 1% additive noise, respectively.

3.1.2 Binomial process pattern without additive noise

Since fabricating a test target for thermal imaging whose contrast follows a Gaussian distribution is difficult in practice, we considered using a target whose contrast followed a binomial distribution. We repeated the method characterized, as shown in Figure 4 the size of the image influence the accuracy of the PSF estimation. We can see that the errors on the estimate of the parameters of the PSF are more accurate for larger target sizes.

3.1.3 Binomial process with additive noise

We repeated the procedure with identical parameters, except for additional 1% additive noise (Figure 5).

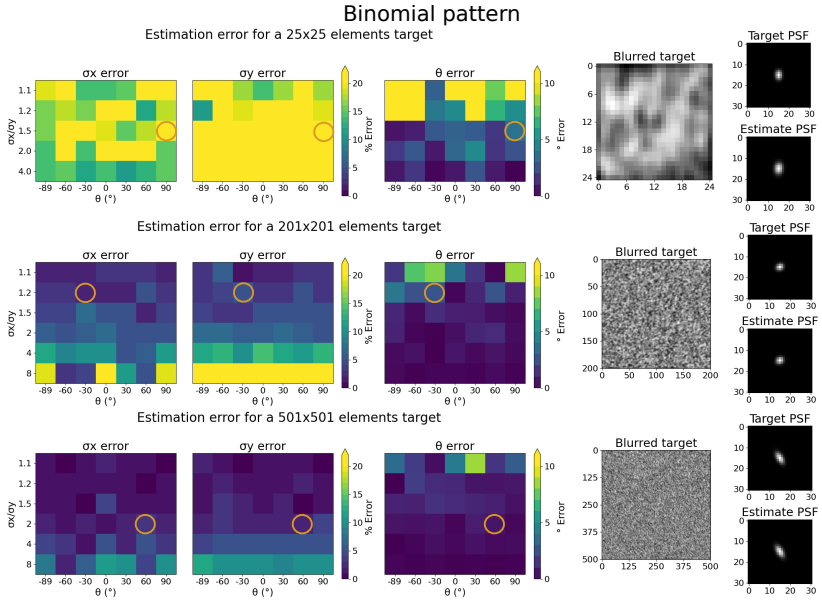

Figure 4: Evaluation of the method for binomial pattern of sizes 25×25, 201×201, and 501×501 pixels. No measurement noise was added. Orange circles indicate parameters for examples on the right.

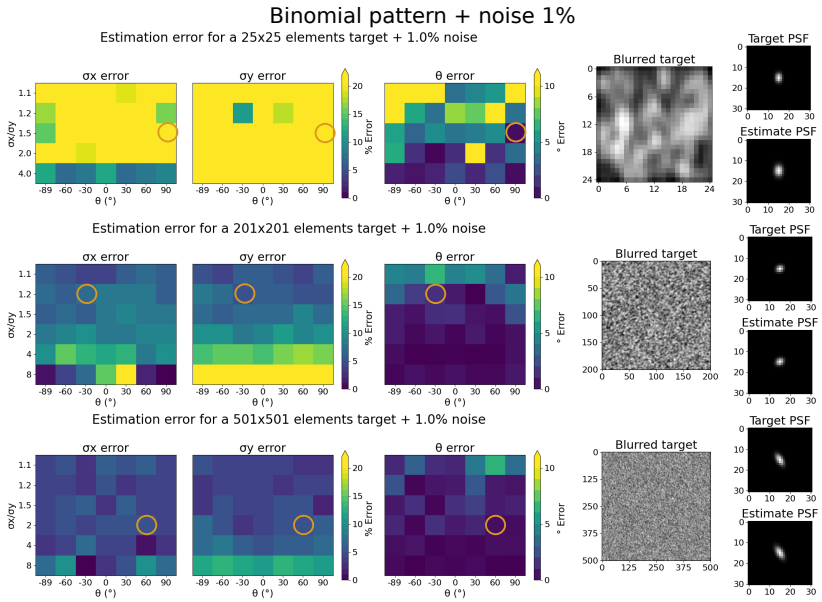

Figure 5: Evaluation of the method for binomial pattern of size 25×25, 201×201, and 501×501 pixels, with 1% additive noise. Orange circles indicate parameters for examples on the right.

3.2 Practical Application

3.2.1 Binomial noise targets cut out in plywood

Since we aim at using the PSF parameter estimation method with thermal imaging devices, we assembled a modular system that allows heating a plain background by placing a terrarium heating mat (ThermoLux heating mat 30×50 cm) between two blank, 5mm-thick plywood boards whose outline matches that of a third board, which was to contain the target. Machine screws hold the cut-out target away from the heated target (Fig. 6).

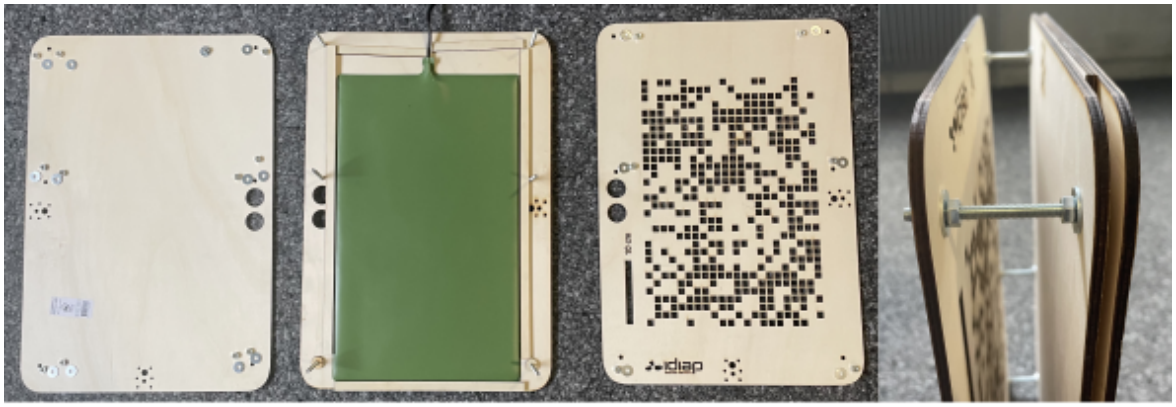

Figure 6: Assembly of the PSF estimation target. The back of the target is made up of two wooden plates with a heating plate between them: (a) middle heating cover panel (b) back panel and heater. The front panel (c) has 1cm-squares cut out according to a binomial distribution pattern. (d) in the assembled target, the pattern is 6cm away from the heating cover panel.

For manufacturing the target, we prepared a vectorial file of the binomial pattern, as shown in Fig. 7 (a) which was used to guide a laser cutter. The assembled target, as viewed from the front is shown in Fig. 7 (b). The square cut-outs are of size 1cm×1cm. Fig. 7 (c) shows a thermal image of the built target with all squares fully resolved. In Fig. 7 (d) the same target is shown as imaged from a distance of 35m, such that the size of one element on the target corresponds to one pixel on the image taken by the camera. That image is used for the PSF parameter estimation.

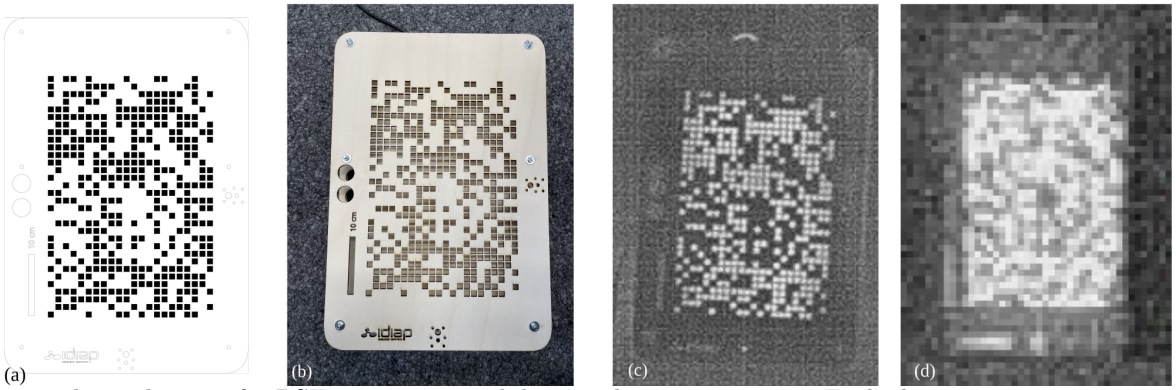

Figure 7: Thermal target for PSF estimation with binomial process pattern. Each element measures 1cm × 1cm.

3.2.2 Experimental illustration

We took images of our heated target using a thermal camera. In one case the camera was kept steady while in the other case we captured the image while moving the camera horizontally to induce motion blur. Next, we applied our PSF estimation algorithm to the images in both cases. As expected, the estimated PSFs reveal circular symmetry in the static case and a shape elongated in the motion direction for dynamic case (Fig.8).

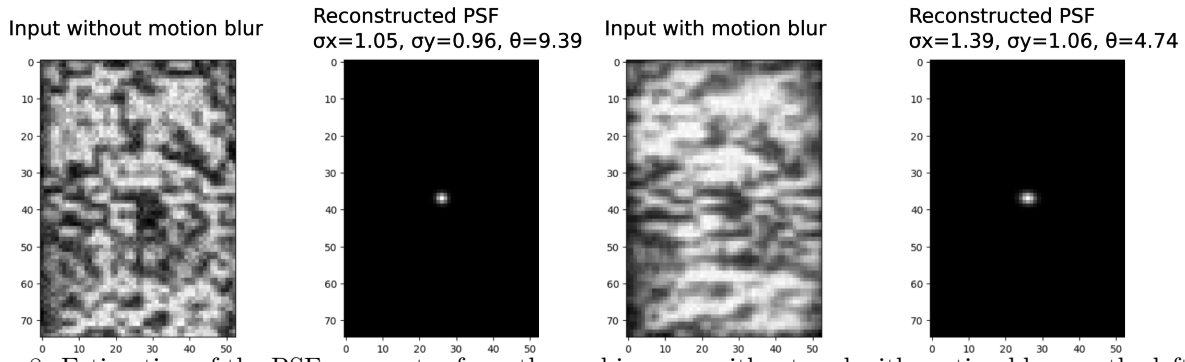

Figure 8: Estimation of the PSF parameter from thermal images, without and with motion blur, on the left and right, respectively

In order to compare the automatically-estimated blur parameters with a visual reference, we built a new target. In addition to a binomial pattern, it also included one half of a Siemens star pattern (Fig. 9 (a)). The Siemens star target pattern can be used to visually evaluate the resolution of optical system and consists of a pattern of spokes that radiate from a central point and widen as they extend outward. In our case, the spokes have a width of 1cm near the center and widen up to 2cm at the outer border, as indicated in Fig. 9 (a).

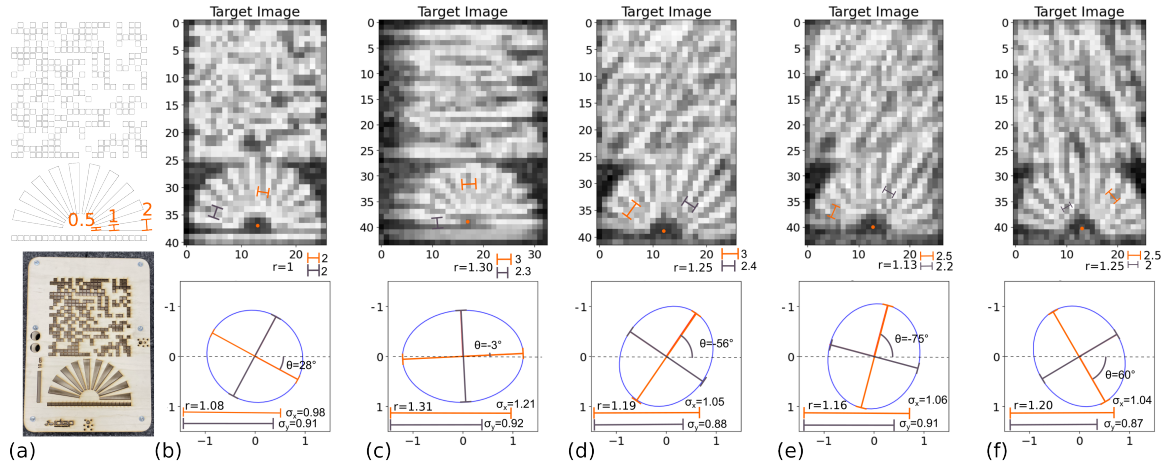

Figure 9: Illustration of automatic PSF estimation from binomial pattern with side-by-side comparison to visual inspection of Siemens resolution star. (a) Binomial target and Siemens star pattern (top) and plywood cut-out (bottom). Dimensions of Siemens star range from 1cm to 2cm. Size of binomial pattern squares is 1cm. (b)–(f) Top row shows measured thermal image. Arrows on Siemens star indicate visually-identified directions of best and worst resolution. The distance from the center of the Siemens star can be used to estimate resolution. Bottom row shows automatically-estimated PSF parameters, represented with an ellipse and its principal axes. In (b) camera and target were static, in (c)–(f) camera was panned during acquisition to generate motion blur.

We first acquired a thermal image while keeping both the camera and target static (Fig. 9(b)). We estimated the parameters using our automatic method on the binomial pattern: $\sigma_x = 0.98$ and $\sigma_y = 0.91$. We visualized these parameters using an ellipse with half-axes corresponding to the parameters. The estimates indicate a fairly

isotropic PSF as the ellipse is nearly round, with a ratio $r = \sigma_x/\sigma_y = 1.08$. The isotropy can be confirmed visually on the Siemens star, which is blurred near the center with similar strength along all directions. For each of two perpendicular directions, we indicated one cycle in the Siemens that we visually identified as characterizing the highest resolved frequencies.

We repeated this experiment but instead of keeping the camera steady during image acquisition, we panned it arbitrarily along various directions, which induced motion blur, as shown on Fig. 9 (b)–(f). The automatic estimate resulted in elongated PSFs, since, unlike in the static case, the blur is directional. We could visually confirm the estimate's directions and ratios on the Siemens star. We indicated two cycles where the resolution appears best and worst by visually identifying the location on the spokes closest and farthest away from the center, respectively, where the star pattern is barely resolved.

The directions of least and best visual resolution are consistent with the directions identified by the automatic algorithm, except for the static case, where the resolution is nearly isotropic, and the direction is therefore less relevant. We note that, as should be expected, when the PSF is elongated along a certain direction, the Siemens star is most blurred along that direction. Visually, this translates to the worst resolution on the Siemens star, the farthest away from the center, being at a 90 degree angle from that direction. Conversely, the narrow direction of the PSF leads to the best resolution on the Siemens star, again oriented at 90 degrees from that direction. We computed the ratios $r = \sigma_x/\sigma_y$ obtained from the automatic PSF parameter estimates and compared them with the ratio between the visually-identified cycle length of the best and worst resolution Fig. 9 (b–f). We found that the ratios and directions were in agreement, with discrepancies of similar magnitude as the estimation errors in the simulations for targets of this size.

4. DISCUSSION

Given the method's simple steps, its computation complexity is mostly dependent on the size $M \times M$ of the window, with typical values ranging from 25×25 to 1000×1000, which determines the complexity of the FFT. The PCA complexity, which is implemented via an Singular Value Decomposition (SVD) of a matrix of small 2×2 matrix, with the number N of sample points influencing the time necessary to generate the point cloud.

The accuracy of the method is dependent on the shape of the PSF. For PSF whose σ_x and σ_y are very different, the estimate of the narrower parameter, in our case always σ_y, is less accurate. When the PSF is round or nearly round, the estimate of the inclination is unreliable, which is to be expected given the inclination is undefined for perfectly round PSFs.

The Siemens star target offers a straightforward alternative to visually estimate the image blur by analyzing the area where the spokes are still distinguishable, providing information about anisotropic resolution as the direction of the blur can be identified visually. Our automated method, applied on experimentally-measured images appears to be effective in determining blur direction and anisotropy and consistent with visual observations of the least and most blurred directions in the Siemens star. As predicted by the simulations on small-scale, 25×25 binomial targets with additive noise shown in Fig.5, only limited accuracy can be expected and increasing the physical target size could improve the accuracy of PSF parameter estimation in the future.

5. CONCLUSION

We described, implemented, and characterized an algorithm that allows estimating the PSF images of textures with values following random distributions.

We also physically implemented this concept by creating test targets to evaluate the method. Finally, we have applied these techniques in the context of imaging models that can be characterized by spatially non-uniform and anisotropic point distribution functions.

The method's simplicity and robust steps, combined with its applicability for thermal imaging could make it a promising method for applications such as non-uniform deconvolution or characterization of local image degradation.

ACKNOWLEDGMENTS

We acknowledge Caspar Henking for his preliminary implementation and study that contributed to this work.

REFERENCES

[1] Grossmann, P., "Depth from focus," *Pattern Recognit. Lett* **5**(1), 63–69 (1987).

[2] Goodman, J. W., [*Introduction to Fourier Optics*], Roberts and Company Publishers (2005).

[3] Zhang, B., Zerubia, J., and Olivo-Marin, J.-C., "Gaussian approximations of fluorescence microscope point-spread function models," *Appl. Opt.* **46**(10), 1819–1829 (2007).

[4] Ehret, T., Davy, A., Morel, J.-M., and Delbracio, M., "Image anomalies: A review and synthesis of detection methods," *Journal of Mathematical Imaging and Vision* **61**, 710–743 (Jun 2019).

[5] Kubota, H. and Ohzu, H., "Method of measurement of response function by means of random chart," *J. Opt. Soc. Amer.* **47**, 666–667 (1957).

[6] Brauers, J., Seiler, C., and Aach, T., "Direct PSF estimation using a random noise target," in [*SPIE Electronic Imaging*], 75370B (2010).

[7] Levy, E., Peles, D., Opher-Lipson, M., and Lipson, S. G., "Modulation transfer function of a lens measured with a random target method," *Appl. Opt.* **38**, 679–683 (Feb 1999).

[8] Shajkofci, A. and Liebling, M., "Spatially-variant CNN-based point spread function estimation for blind deconvolution and depth estimation in optical microscopy," *IEEE Trans. Image Proces.* **29**, 5848–5861 (2020).

[9] Piras, F., De Moura Presa, E., Wellig, P., and Liebling, M., "Local estimation of parametric point spread functions in thermal images via convolutional neural networks," in [*Target and Background Signatures VIII*], Stein, K. and Schleijpen, R., eds., **12270**, 1227009, International Society for Optics and Photonics, SPIE (2022).